Chemosphere 291 (2022) 132738

Contents lists available at ScienceDirect

Chemosphere

journal homepage: www.elsevier.com/locate/chemosphere

On the behaviour of Atrazine removal from water using fabrics as anodes and cathodes

Hanene Hamous [a], Aicha Khenifi [a], Francisco Orts [b], José Bonastre [b], Francisco Cases [b,*]

[a] Physical and Chemical Laboratory of Materials, Catalysis and Environment (LPCMCE) Faculty of Chemistry University of Sciences and Technology of Oran (USTO M-B), BP 1505, Oran, Algeria

[b] Departamento de Ingeniería Textil y Papelera, EPS de Alcoy, Universitat Politècnica de València, Plaza Ferrándiz y Carbonell s/n, 03801, Alcoy, Spain

HIGHLIGHTS

- Modified textile electrode permits efficient wastewater treatments.
- Very low energy consumption needed for 90% Atrazine electrochemical degradation.
- High current efficiency is observed when the undivided cell is used with chloride.
- These electrodes are a valuable alternative for wastewater remediation.

GRAPHICAL ABSTRACT

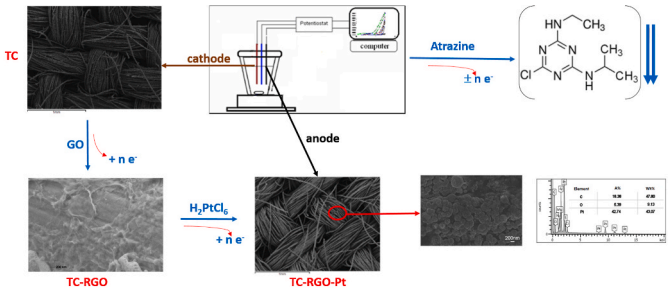

ARTICLE INFO

Handling Editor: E. Brillas

Keywords:
Textile electrodes
Graphene
Platinum nanoparticles
Pesticides
Atrazine
Electrochemical degradation

ABSTRACT

This study examines the degradation of atrazine (ATZ) with Pt-modified textile electrodes using an electrochemical method that is comparatively studied in two electrochemical cell configurations: cells with separated anodic and cathodic compartments (divided configuration); and without any separation (undivided configuration). The influence of the presence of chloride ions was studied. The best results were obtained when an undivided cell was used. The morphology and composition of the dispersed Pt coatings were analyzed using field emission scanning electron microscopy (FESEM) and Energy Dispersive X-Ray Analysis. The FESEM analyses confirmed that the textile surface was effectively modified by the electrocatalytic material. High performance liquid chromatography, gas chromatography mass spectrometry, and spectroscopic methods were used to follow the evolution of major oxidation products. Total organic carbon, chemical oxygen demand, and total nitrogen were used to evaluate the degradation efficiency of treated aqueous solutions. The experimental results obtained indicate that the efficiency of the electrochemical treatment was high with a low energy consumption when using electrodes based on textile materials, such as anodes or as cathodes (in particular, in electrolysis without compartment separation). All these can be produced at very competitive prices.

* Corresponding author.
E-mail address: fjcases@txp.upv.es (F. Cases).

https://doi.org/10.1016/j.chemosphere.2021.132738
Received 29 July 2021; Received in revised form 21 October 2021; Accepted 28 October 2021
Available online 28 October 2021

Table 1
Electrooxidation performance in the treatment of Atrazine.

(Anode-cathode)	Optimal operating conditions	Results and comments	References
Ti/($IrSnO_2$)–Pt Ti/($IrRuSnO_2$) –Pt	T = 25 °C, [Na_2SO_4] = 0.033 M or [NaCl] = 0.1 M, J = 40 mA cm^{-2}, $[ATZ]_0$ = 20 mg L^{-1}	**After 120 min of treatment**: 16.69 and 100% degradation; 4.24 and 30.94% of TOC; 125.9 and 1.25 $kWhm^{-3}$ $order^{-1}$ electrical energy per order were obtained in 0.033MNa_2SO_4 and 0.1NaCl respectively with Ti/($IrSnO_2$) anode 24.63 and 100% degradation; 5.25 and 30.83% of TOC; 81.47 and 81.47 1.33 $kWhm^{-3}$ $order^{-1}$ electrical energy per orderwere obtained in 0.033MNa_2SO_4 and 0.1NaCl respectively with Ti/($IrRuSnO_2$) anode	Malpass et al. (2006)
Pt–Pt	T = 25 and 60 °C, J = 70 mA cm^{-2}, $[ATZ]_0$ = 0.05 mM	At 25 °C atrazine is partially degraded and At 60 °C, atrazine is degraded completely to cyanuric acid in 4 h of electrolysis	Mamián et al. (2009)
BDD-stainless steel	T = 35 °C, pH = 3, [Na_2SO_4] = 0.05 M , J = 100 mA cm^{-2}, $[ATZ]_0$ = 30 mg L^{-1}	90% degradation and 90% TOC after 360 min, with 20% MCE	Borràs et al. (2010)
Ti/(IrO_2)–Ti Ti/(SnO_2)-Ti	T = 25 °C, pH = 5, [NaCl] = 1 g L^{-1}, I = 2 A, $[ATZ]_0$ = 100 µg L^{-1},	95 and 75% degradation with Ti/IrO_2 and Ti/SnO_2 anode respectively	Zaviska et al. (2011)
BDD-carbon filter	T = 25 °C, pH = 6.7, [Na_2SO_4] = 0.1 M, J = 40 mA cm^{-2}, $[ATZ]_0$ = 0.1 M	Degradation of 97% and 97% of TOC after 480 min	Oturan et al. (2012)
BDD-Pt	T = 25 °C,pH = 3, [Na_2SO_4] = 0.033 M or [NaCl] = 0.05 M, J = 40 mA cm^{-2}, $[ATZ]_0$ = 20 mg L^{-1}	After 300 min of treatment, 80% mineralization, 9% mineralization current efficiency and 1.93 kW h g^{-1} TOC energy cost were obtained	Garza-Campos et al. (2014)
Ti/(RuO_2)$_{0.5}$–(Sb_2O_5)$_{0.5}$-Pt Ti/(RuO_2)$_{0.8}$–(Sb_2O_5)$_{0.2}$-Pt	T = 25 °C, [Na_2SO_4] = 0.1 M, J = 10 and 20 mA cm-2, [ATZ] 0 = 10 mg L^{-1}	Degradation of 98% after 100 min	Santos et al. (2016)
BDD-graphite	T = 25 °C, pH = 6, [Na_2SO_4] = 0.03 M, J = 2 mA cm^{-2}, [ATZ]0 = 100 µgL^{-1}	Degradation of 94.7% and 93% of TOC after 240 min	Komtchou et al. (2017)

1. Introduction

Phytosanitary products used in agriculture are degrading the environment, particularly through the contamination of surface and groundwater. These compounds are used to kill harmful species and weeds that damage crops and agricultural products. Various studies reveal the presence of numerous pesticides in surface water and Atrazine is one of the most common pesticides detected in surface water and groundwater (Hildebrandt et al., 2008; Reilly et al., 2012) and is widely used around the world (Su and Zhu, 2006). Atrazine is used mainly to fight weeds and grass weeds that harm the growth of corn, rapeseed, and lowbush blueberries. It is also used for general weed control in non-crop and industrial areas. Atrazine is a potential endocrine-disrupting compound that induces complete feminization of amphibians such as *Xenopus laevis* (Hayes et al., 2010) and presents a risk to human health (MacLennan et al., 2003). The use of this herbicide is restricted in many countries nowadays (He et al., 2019). The maximum concentration of atrazine in primary drinking water in the United States is 3.0 µgL^{-1} (Aggelopoulos et al., 2018). The European Community also lists atrazine as one of the drinking water testing indicators, and it stipulates that the mass concentration should not exceed 0.1 µgL^{-1} (Hou et al., 2017). In China, according to the Surface Water Environmental Quality Standard (GB3838-2002), the maximum allowable concentration of atrazine in surface water is 3.0 µgL^{-1}, and in the Water Quality Standard for Urban Water Supply (CJ/T 206–2005), the limited concentration of atrazine is 2.0 µgL^{-1}. Despite these regulations, ATZ have been reported to exceed the recommended value in many countries (Dorsey, 2003). Today, many techniques exist to treat waters loaded with Atrazine. The most used techniques include membrane filtration (Gkementzoglou et al., 2016), adsorption (Cao and Harris, 2010; Liu et al., 2015), chemical oxidation (Lutze et al., 2015; Bu et al., 2017; Luo et al., 2017) and ozonation (Hapeman-Somich et al., 1992). However, most of these techniques produce secondary wastes, such as spent adsorbent, retentate in adsorption and membrane treatment and non-reactive sludge in biological reactive sludge in biological treatment. Due to the tightening of environmental legislation, new waste-free technologies are needed (He et al., 2019). Faced with this worrying situation the scientific community is mobilizing and working on the implementation of innovative processes to treat these bioremediation pollutants. It is in this search for an effective solution to these emerging pollutants that electrochemical processes have appeared. In this process, OH• radicals are produced from the oxidation of water on the surface of an anode with a strong oxygen release overvoltage. This technique is attractive because it offers several distinct advantages such as its versatility, high energy efficiency, ease of automation, and low cost. The major reagent is the electron itself (Yan et al., 2014). In addition, the electrochemical process can treat a wide range of organic compounds refractory to biological treatments (Radjenovic and Sedlak, 2015).

Examination of the data in Table 1 shows that the nature of the electrode strongly contributes to the efficiency of electrochemical oxidation of Atrazine in aqueous solutions (Zhou et al., 2011), including BDD-graphite (Komtchou et al., 2017), Ti/Ru0·3Ti0·7O_2 (Malpass et al., 2006), BDD-stainless steel (Borràs et al., 2010); Ti/(RuO_2)$_{0.5}$–(Sb_2O_5)$_{0.5}$-Pt (Santos et al., 2016), Ti/(RuO_2)$_{0.8}$–(Sb_2O_5)$_{0.2}$-Pt

(Santos et al., 2016); BDD-carbon filter (Oturan et al., 2012); Ti/(IrO_2)–Ti (Zaviska et al., 2011), Ti/(SnO_2)-Ti (Zaviska et al., 2011); Pt–Pt (Mamián et al., 2009); and BDD-Pt (Garza-Campos et al., 2014).

The type of electrodes to be used in an electrochemical process is of paramount importance because the efficiency of the treatment depends on the performance of the electrodes. The ideal electrode material for organic degradation of pollutants would have the following qualities: complete physical and chemical stability in the electrolysis medium; corrosion resistance; high electrical conductivity; exposure more oriented to the degradation of organic pollutants than to the production of secondary reactions; and a low cost-to-lifetime ratio (Anglada et al., 2009; Panizza, 2010).

Carbon materials such as activated carbon textiles are widely used as supports for active transition metals owing to their large surface area and outstanding electronic conductivity (Nie et al., 2012). Recently, graphene is one of the most promising materials for the development of electrodes. This 2D material exhibits exceptional mechanical, electrical, and thermal properties. Graphene has opened the way to new perspectives in fields as varied as electronics and energy storage and is currently one of the most studied materials (Li and Kaner, 2008).

Graphene has been often described as the material of the future. Recently graphene oxide (GO) and its reduced graphene oxide (RGO) possess wide attention because of its high surface area and less cost (Wang et al., 2009; Li et al., 2010; Luo et al., 2012; Ren et al., 2014). These unique features make graphene attractive as a promising carrier for Pt particles and with the potential to enhance electrocatalytic activity (Ding et al., 2019). Consequently, RGO could serve as a good linker to bridge the gap between carbon cloth and noble metals. Moreover, it has been demonstrated in previous papers that the presence of RGO coatings strongly decreases the degradation of the textile carbon electrodes surface in comparison with the absence of such RGO coating. (Fernández et al., 2017; Hamous et al., 2021).

The objective of this study is to conjugate these two carbon materials to develop high efficient modified textile electrodes. These electrodes have been explored for eliminating Atrazine by oxidation, reduction, and oxidation-reduction. These electrodes have also shown their efficiency in the electrochemical degradation of azo dye “OrangeG” (Hamous et al., 2021). Moreover, these 2D electrodes exhibit a dimensional versatility that could be useful for the development of electrochemical cells that could treat a higher volume of wastewater with low costs and low energy consumption.

2. Experimental section

2.1. Materials and reagents

ATZ (solubility in water 33 mg L^{-1} at 25 °C) was purchased in the highest purity available from Riedel-de Haën. It was used without any further purification. Chemicals were reagent grade and purchased from Merck and Fluka Scientific. Monolayer GO powders were purchased from Nanoinnova Technologies SL (Spain). The platinum wire is commercially available and with a purity of 99.99 w %. FlexzorbTM FM10 activated carbon fabrics electrodes were obtained from Chemviron Carbon. The water used throughout the experiments with resistivity >18.2 MΩ cm was obtained using a Millipore Milli-Q system.

2.2. Characterization

The decay in atrazine concentration was monitored by HPLC using an ultraviolet–visible spectrometry diode array detector Hitachi Elite Lachrom Chromatographic system set at $\lambda = 266$ nm with high sensitivity that reduces noise to 1.5 10^{-5} AU or less and wavelength accuracy of 1 nm; fitted with a Lichrospher 100RP-18C column (5 μmpacking). Analyses were carried out by using the mobile phase: methanol (eluent A) and aqueous buffer solution NaH_2PO_4–Na_2HPO_4 with pH = 6.9 (eluent B). The flow rate was 1 mL min^{-1} and the injection volume was 80 μL.

A Shimadzu TOC-VCSN analyzer based on the combustion-infrared method was used to measure TOC and TN, equipped with high sensitivity measurements kit options: 4 μg/L. A digester apparatus (Spectroquant® TR320) and a test analyzer (Spectroquant® NOVA) were used for COD measurements with a measuring range of 50–500 mg L^{-1} COD.

GC-MS analysis was performed in electron ionization mode using a Shimadzu GC–MSQP2010 gas chromatograph-mass spectrometer (GC–MS) equipped with a secondary electron multiplicator dynode (MSD). The sensitivity of the equipment is: S/N > 60/1 (RMS) for 100 fg octafluoronaphthalene molecular ion at *m/z* 272. A Teknokroma S Meta X5, P/N TR-820232 capillary column (30 m × 0.25 mm × 0.25 μm) was used. The solutions before analysis were treated as follows: 25 mL atrazine treated solutions were extracted with a total volume of 100 mL (40 mL + 30 mL + 30 mL) of dichloromethane three times. The extracts were concentrated around 100 μL under a slow stream of dry nitrogen and then injected into the GC-MS. The column was held at 90 °C for 0.5 min, then a temperature gradient program at 15 °C min^{-1} was used from 90 °C to 160 °C. Then from 160 °C to 280 °C to 25 °C min^{-1}. Finally; the temperature was held at 280 °C for 5 min (Ma et al., 2003). The temperature of the injection part and the MS transfer line was 280 °C. Helium was used as a carrier gas at a flow rate of 1.5 mL min^{-1}. Mass spectra were acquired in the electron impact mode. The *m/z* scan was from 45 to 300 with a transfer line temperature of 300 °C.

2.3. Electrodes synthesis

All electrochemical experiences were carried out in a cone-shaped voltammetric cell using a three-electrode system with a potentiostat/galvanostat Autolab PGSTAT30 under ambient conditions. An Ag/AgCl (sat. KCl) electrode was used as the reference. The cyclic voltammetry was performed at various scan rates. The working electrode was prepared by immersing a carbon textile electrode in a solution 3 g.L^{-1} of GO in 0.1 M $LiClO_4$. Electrodeposition was carried cycling between −1.6 V and 0.6 V during 20 cycles at a scan rate of 20 mV s^{-1}. After RGO is electrodeposited the electrode is immersed in a second solution containing 5 mM H_2PtCl_6 and 0.5 M H_2SO_4. The potential range used was from +0.4 V to −0.25 V using a scan rate of 10 mV s^{-1}. The electrodes obtained by this method were named with the abbreviation TC-RGO-Pt. A Pt wire and a cylindrical stainless-steel mesh 4.5 cm high by 3.5 cm wide were used as counter electrodes for electrodeposition of reduced graphene oxide (RGO) and Pt nanoparticles respectively. Before each experiment, the solutions were deaerated with N_2 for 30 min. After the electrode synthesis, the electrode was dried for 24 h at room temperature.

2.4. Electrolysis of 0.1 mM atrazine solution

The initial concentration of ATZ in water was 0.1 mM or 21 mg L^{-1} (very close to the limit of solubility). Similar or higher concentrations to 21 mg L^{-1} have been studied by several researchers (Malpass et al., 2006, 2013; Balci et al., 2009; Borràs et al., 2010; Garza-Campos et al., 2014). The electrolysis processes were carried out at controlled potential. The selected potentials must be within the range of electrochemical reactivity that appears on the current-potential curves plotted by cyclic voltammetry. Two series of electrolysis were carried out: one in a divided cell (H shape) with anodic and cathodic compartments separated by a cationic membrane (Nafion 117 from DuPont) and the other an undivided cell. The undivided electrochemical cell was equipped with a TC-RGO-Pt anode placed in the centre of the electrochemical reactor. To obtain a good potential distribution, a TC cathode was immersed parallel to the anode. The volume of the solution was 50 mL. In the undivided cell, the anodic compartment containing the TC/RGO/Pt anode is immersed in 50 mL solution with Atrazine, whereas the cathodic one containing the Pt wire is immersed in 50 mL solution of the same background electrolyte free of Atrazine. The

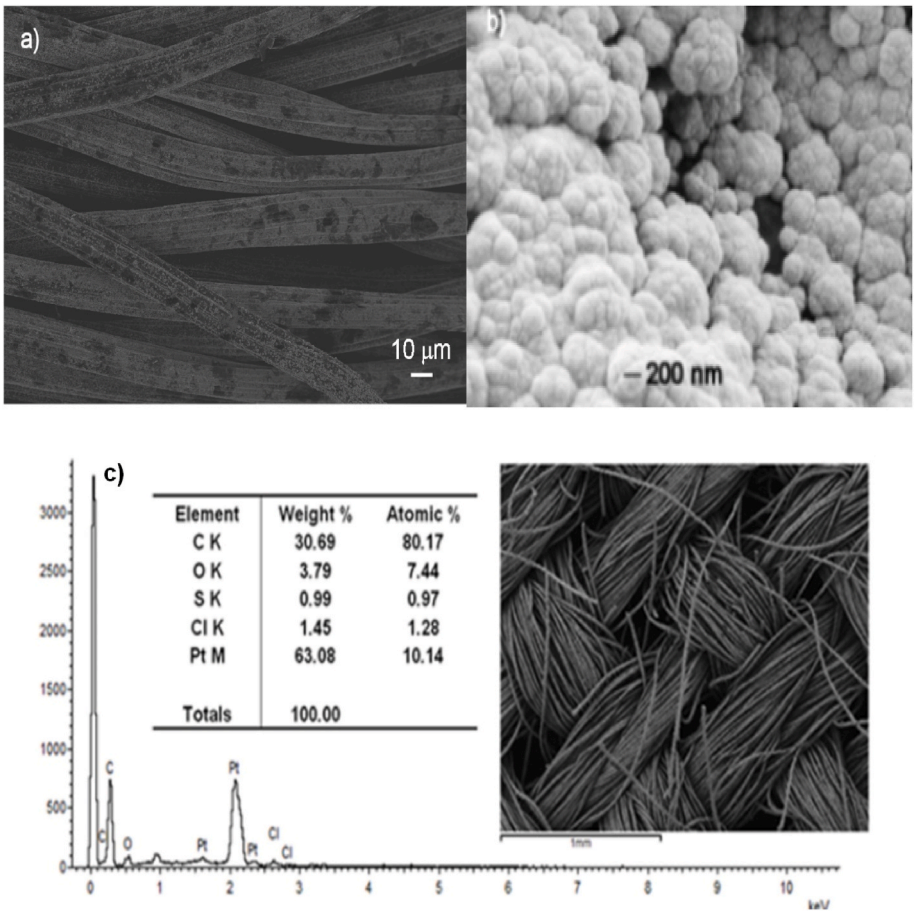

Fig. 1. a) and b) FE–SEM images showing the morphology for the synthesized TC–RGO–Pt electrode c) EDX surface analysis.

potential was controlled by a Gamry 1000 potentiostat-galvanostat, and the counter-electrode potential was measured with a digital multimeter. In all the assays, the solution was vigorously stirred with a magnetic bar at 250 rpm to ensure good homogenization of the solution and the transport of the organic matter towards/from the electrodes. To follow the degradation kinetics of the molecules and the evolution of the organic matter, and to determine the resulting products, as well as the composition of the solutions, samples of 1 mL were taken at regular intervals for chromatographic analysis. Experimentally, the degradation efficiency of Atrazine was followed from the abatement of their TOC, TN, and COD decreases, the average current efficiency (ACE), and the electrical energy consumption per order (EEO).

The average current efficiency for each potential could be calculated from COD results following the equation (Panizza and Cerisola, 2009).

$$ACE = \frac{COD_0 - COD_t}{8\ I\ t} F V\ \ 100 \tag{1}$$

where COD_0 and COD_t are the chemical oxygen demands at electrolysis times 0 and t, respectively (g O_2 L^{-1}), F is the Faraday constant (96,487 C mol^{-1}), V represent the volume of the electrolyte (L), 8 is the oxygen equivalent (g eq^{-1}), I is the current (A) and t is the degradation time (s).

The electrical energy per order (EE/O) is the electrical energy in kilowatt-hour (kWh) required to bring about a reduction by one order of magnitude in the concentration of the contaminant (C) in a unit of volume of contaminated water. The EE/O (kWh m^{-3} $order^{-1}$) can be calculated from the following equation (Bolton et al., 2001).

$$EEO = \frac{P\ t}{V\ \log\left(\frac{A_i}{A_f}\right)} \tag{2}$$

where: P is the rated power (kW) (P = I V), t is the time of electrolysis (h), V is the volume treated (L), A_i and A_f are the initial and final areas of the chromatographic peak associated with the pollutant of interest.

3. Results and discussion

3.1. Microstructural characterization of TC-RGO-Pt

FESEM was used to observe the morphology of the coatings obtained and the distribution of Pt nanoparticles. Fig. 1 shows the FESEM micrographs and the EDX analysis of the TC-RGO-Pt electrode obtained by cyclic voltammetry. In this image, the presence of spherical Pt nanoparticles electrodeposited on the electrode is visible. Quite uniform distribution and a well dispersed Pt is observed. The Pt nanoparticles cover almost the entire surface of the electrode homogeneously without discontinuity (uncoated areas).

EDX permit the identification of the chemical elements present on the TC-RGO-Pt electrode surface and their relative content. The spectrum given in Fig. 1c identified C, O, and Pt as the main elements on the electrode surface.

3.2. Atrazine degradation during the electrolysis

The voltammogram plotted with a TC-RGO-Pt electrode immersed in a solution of 0.1 mM Atrazine did not show any characteristic oxidation peak. Moreover, neither did the voltammogram obtained with a Pt electrode show a clear oxidation peak associated with Atrazine, although it did show an oxidation wave up to 1.5 V (where oxygen evolution starts) with the middle of the wave at around 1.3 V (figures not shown). We can, under these conditions, work on the whole range of

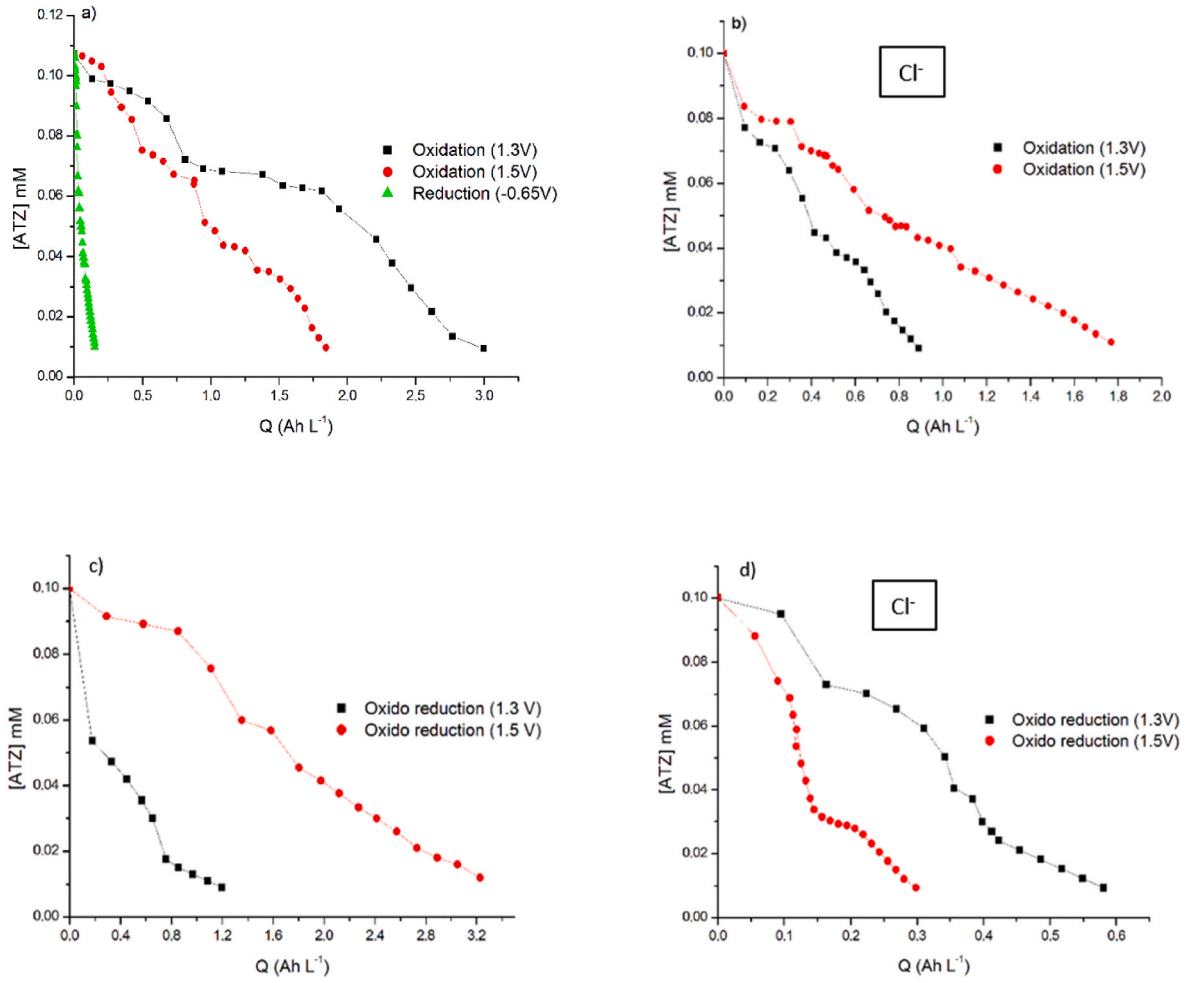

Fig. 2. Variation of Atrazine concentrations versus loaded specific charge during electrolysis with TC-RGO-Pt/Pt as anode and TC as cathode in a) 50 (mM) Na_2SO_4 in a divided cell, b) 50 (mM) Na_2SO_4 + 5 mM NaCl in a divided cell, c) 50 (mM) Na_2SO_4 in an undivided cell and d) 50 (mM) Na_2SO_4 + 5 (mM) NaCl in an undivided cell.

potential examined. In oxidation, the influence of potential is more significant than in reduction. Our results have shown that a potential of 1.3V is sufficient to degrade Atrazine.

By measuring the decrease of chromatographic peak area during electrolysis, it is possible to calculate the decrease of the atrazine concentration as a function of the specific charge (Fig. 2). This evolution is strongly influenced by both the nature of the electrochemical cell and the supporting electrolyte. The highest removal rate is obtained when reduction and oxidation-reduction (undivided cell) are done in the presence of chloride.

Table 2
Evolution of different parameters when 90% of Atrazine is removed after the electrolysis as a function of the experimental parameters.

Cell	Electrolyte	Potential V	Q Ah L^{-1}	TOC %	TN %	COD %	ACE %	EEO kWh m^{-3} $order^{-1}$
Divided Cell								
	50 mM Na_2SO_4	1.30	3.00	2.87	3.38	2.40	1.7	3.85
	50 mMNa_2SO_4+5mM NaCl	1.30	0.89	11.02	12.83	2.32	5.0	1.15
	50 mMNa_2SO_4	1.50	1.84	2.18	41.41	2.41	3.1	2.77
	50 mMNa_2SO_4+5mM NaCl	1.50	1.77	2.41	30.68	1.12	1.9	2.65
	50 mMNa_2SO_4	-0.65	0.15	1.68	8.13	1.60	1. 0	0.10
undivided Cell								
	50 mMNa_2SO_4	1.30	1.2	34.39	52.07	4.79	8.4	1.56
	50 mMNa_2SO_4+5mM NaCl	1.30	0.58	12.82	42.43	8.96	27.7	0.75
	50 mMNa_2SO_4	1.50	3.23	9.41	43.44	3.51	2.3	4.8
	50 mMNa_2SO_4+5mM NaCl	1.50	0.30	2.57	33.49	6.65	11.3	0.45

The increase in the rate of atrazine removal after oxidation in the presence of chloride ions for both electrochemical cells and the two potential values (1.3 and 1.5 V) used in the experiences shown in the figures can be explained by the formation of different oxidizing agents and the degradation of organic matter at the electrode by hydroxyl radical (·OH) reactions (3) to (5) and also by chemical reaction with the active chlorine formed in the solution according to reactions (6) and (7) (Garcia-Segura et al., 2018):

$$H_2O + M \rightarrow M(OH^{\cdot}) + e \quad (3)$$

$$M(OH^{\cdot}) \rightarrow MO + H^{+} + e \quad (4)$$

$$MO + R \rightarrow M + products \quad (5)$$

$$2Cl^{-} \rightarrow Cl_{2(aq)} + 2\acute{e} \quad (6)$$

$$Cl_{2(aq)} + H_2O \rightarrow HClO + Cl^{-} + H^{+} \quad (7)$$

Moreover, the efficiency of Na_2SO_4 can be explained by the contribution of sulfate oxidizing species to the degradation process (Fig. 2a and c). Indeed, although HO· generated at the anode surface is primarily responsible for the oxidation of Atrazine, when Na_2SO_4 is used in the solution as the electrolyte, sulfate radicals generated in solution, according to the reactions (8)–(10), may also participate in the oxidation (Murugananthan et al., 2011):

$$2SO_4^{2-} \rightarrow S_2O_8^{2-} + 2\acute{e} \quad (8)$$

$$HO^{\cdot} + SO_4^{2-} \rightarrow SO_4^{\cdot -} + HO^{-} \quad (9)$$

$$SO_4^{\cdot -} + SO_4^{\cdot -} \rightarrow 2S_2O_8^{2-} \quad (10)$$

In the case of Fig. 2c and d an increase in the electrolysis potential not only produce an increase of the active chlorine generated, but also an increase in the rate of other reactions that decrease the ACE (see Table 2) of the main reaction (as oxygen evolution). Moreover, an increase in the reduction rate occurs because of the increase in the reduction potential of the counter electrode (the cathode in these experimental conditions). This last fact is so relevant as can be seen in the rate of degradation of the ATZ under reduction conditions (Fig. 2a). The absence of a reduction mechanism is the explanation of why the effect of potential is opposite when only oxidation occurs in the presence of sodium chloride as an electrolyte (Fig. 2b). When using an undivided cell, the organic material is oxidized by M (OH·) formed on the anode surface and, at the same time, is reduced in the cathode. In this case, some of the intermediates generated by oxidation are reduced on the cathode surface. Moreover, there is a synergy between oxidation and reduction because both processes are efficient in Atrazine removal.

3.3. Total organic carbon (TOC), chemical oxygen demand (COD), and total nitrogen (TN) analyses

Table 2 shows the percentage values of TOC, TN, and COD removed at loaded charges correspond to the values obtained when 90% of Atrazine is removed (see Fig. 2). The more noticeable results are highlighted. The removal of Atrazine increase when the undivided cell is used. Less loaded charges correspond to a higher % of TOC, TN, and COD removed. In other words, not only the ohmic drop decreases when the use of a membrane is avoided, but a good synergy occurs between oxidation and reduction processes of the organic matter and their intermediates.

Moreover, Table 2 highlights the more noticeable contribution of divided and undivided cells towards electrical energy consumption and average current efficiency. As can be observed, the lowest energy consumption occurs after reduction and the highest efficiency occur after oxidation in electrolysis without compartment separation.

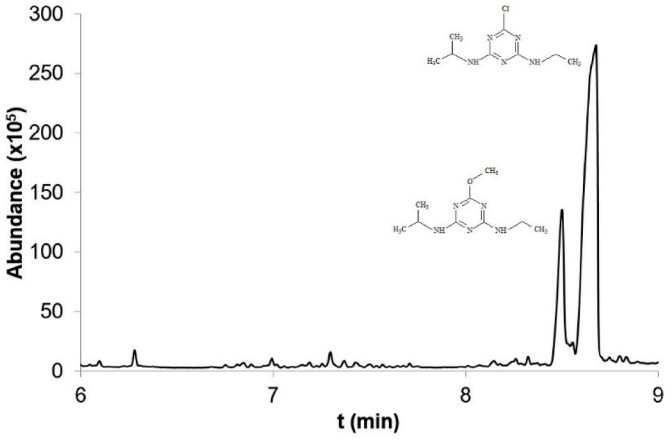

Fig. 3. GC chromatograms of Atrazine solution treated by undivided cell electrolysis at 1.5 V with 50 (mM) Na_2SO_4 + 5 (mM) NaCl. Chromatographs peaks are assigned by MS analyses.

3.4. GC-MS analyzes

GC-MS analyzes were performed for the solutions obtained after oxidation with chloride with the two cell configurations. All samples showed similar results. Two compounds were identified: Atrazine (the fraction of the original undegraded compound) and Atrazine-methoxy (1,3,5-Triazine-2,4-diamine-N-ethyl-6-methoxy-N'-(1-methylethyl). This latter compound comes from the replacement of the chlorine atom by a methoxy group in the Atrazine molecule. The Atrazine molecule is oxidized and a methyl group is added to its molecular structure. Fig. 3 shows the GC chromatogram of the Atrazine solution treated by undivided cell electrolysis at 1.5 V with 50 mM Na_2SO_4 + 5 mM NaCl. This treatment provides the best overall results for ACE and EEO parameters as shown in Table 2. The two compounds remain in solution after the electrochemical treatment are observed.

3.5. Atrazine degradation mechanism

The chromatographic and spectroscopic results of the aqueous atrazine solution after the electro-oxidation treatment allowed us to propose a scheme (Fig. 4) that resumes the composition of the solution after the degradation of atrazine under the applied experimental conditions.

4. Conclusions

The textile carbon electrodes modified by RGO and nanoparticles of Pt developed by our research group present a good behaviour for the degradation of emerging pollutants, in this case, phytosanitary products. In all the cases studied in this research, the loaded charge needed to decrease 90% of the initial organic matter is very low and this highlights the reduction treatment and the oxide-reduction (undivided process). Nevertheless, the reduction treatment did not enable a greatly extended degradation of the molecular structure of the organic pollutant. This degradation occurs across a wide extension when oxidation and especially oxidation-reduction are applied.

The current efficiency of the undivided process with chloride is the highest obtained in the applied experimental conditions. In all cases, the energy consumption is competitive with that of the other electrodes usually used in the electrochemical treatments of pollutants. Once again the configuration is undivided when chloride is present, and this shows the lowest energy consumption (0.45 kWh m^{-3} $order^{-1}$).

In conclusion, the use of a textile 2D electrode, dimensionally versatile, with a great relation of area/mass and area/volume enable us the development of compact electrochemical reactors used in water

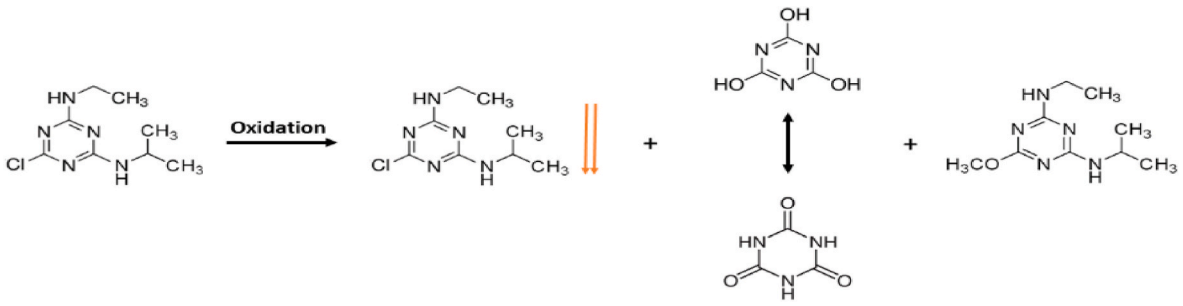

Fig. 4. A scheme that resumes the molecules detected after the atrazine electrooxidation process.

remediation with a competitive efficiency and cost. So, a novel design is now in progress.

Declaration of competing interest

The authors declare that they have no known competing financial interests or personal relationships that could have appeared to influence the work reported in this paper.

Acknowledgements

Spanish Agencia Estatal de Investigación (AEI) and European Union (FEDER funds) are acknowledged for the financial support (contracts MAT 2016-77742-C2-1-P and CTQ 2017-90659-RED). Chemviron Carbon who kindly donated the FlexzorbTM FM10 activated carbon fabrics and Funding for open access charge, CRUE-Universitat Politècnica de València, are acknowledged too.

Appendix A. Supplementary data

Supplementary data to this article can be found online at https://doi.org/10.1016/j.chemosphere.2021.132738.

Authors contribution statement

Hanene Hamous: Investigation, Writing – original draft, Writing -review & editing, Visualization; Aicha Khenifi: Conceptualization, Methodology, Writing – review & editing; Francisco Orts: Investigation; José Bonastre: Investigation, Writing – review & editing; Francisco Cases: Supervision, Writing – review & editing, Investigation.

References

Aggelopoulos, C.A., Tataraki, D., Rassias, G., 2018. Degradation of atrazine in soil by dielectric barrier discharge plasma–Potential singlet oxygen mediation. Chem. Eng. J. 347, 682–694.

Anglada, A., Urtiaga, A., Ortiz, I., 2009. Contributions of electrochemical oxidation to waste-water treatment: fundamentals and review of applications. J. Chem. Technol. Biotechnol. 84, 1747–1755.

Balci, B., Oturan, N., Cherrier, R., Oturan, M.A., 2009. Degradation of atrazine in aqueous medium by electrocatalytically generated hydroxyl radicals. A kinetic and mechanistic study. Water Res. 43, 1924–1934.

Bolton, J.R., Bircher, K.G., Tumas, W., Tolman, C.A., 2001. Figures-of-merit for the technical development and application of advanced oxidation technologies for both electric-and solar-driven systems (IUPAC Technical Report). Pure Appl. Chem. 73, 627–637.

Borràs, N., Oliver, R., Arias, C., Brillas, E., 2010. Degradation of atrazine by electrochemical advanced oxidation processes using a boron-doped diamond anode. J. Phys. Chem. 114, 6613–6621.

Bu, L., Bi, C., Shi, Z., Zhou, S., 2017. Significant enhancement on ferrous/persulfate oxidation with epigallocatechin-3-gallate: simultaneous chelating and reducing. Chem. Eng. J. 321, 642–650.

Cao, X., Harris, W., 2010. Properties of dairy-manure-derived biochar pertinent to its potential use in remediation. Bioresour. Technol. 101, 5222–5228.

Ding, Y., Zheng, H., Cheng, J., Xu, H., Sun, M., Yan, G., 2019. Platinum supported on reduced graphene oxide as a catalyst for the electrochemical hydrogenation of soybean oils. Solid State Sci. 92, 46–52.

Dorsey, A., 2003. Toxicological Profile for Atrazine. Agency for Toxic Substances and Disease Registry.

Fernández, J., Bonastre, J., Molina, J., del Río, A.I., Cases, F., 2017. Study on the specific capacitance of an activated carbon cloth modified with reduced graphene oxide and polyaniline by cyclic voltammetry. Eur. Polym. J. 92, 194–203. https://doi.org/10.1016/j.eurpolymj.2017.04.044.

Garcia-Segura, S., Ocon, J.D., Chong, M.N., 2018. Electrochemical oxidation remediation of real wastewater effluents—a review. Process Saf. Environ. Protect. 113, 48–67.

Garza-Campos, B.R., Guzmán-Mar, J.L., Reyes, L.H., Brillas, E., Hernández-Ramírez, A., Ruiz-Ruiz, E.J., 2014. Coupling of solar photoelectro-Fenton with a BDD anode and solar heterogeneous photocatalysis for the mineralization of the herbicide atrazine. Chemosphere 97, 26–33.

Gkementzoglou, C., Kotrotsiou, O., Koronaiou, M., Kiparissides, C., 2016. Development of a sandwich-type filtration unit packed with MIP nanoparticles for removal of atrazine from water sources. Chem. Eng. J. 287, 233–240.

Hamous, H., Khenifi, A., Orts, F., Bonastre, J., Cases, F., 2021. Carbon textiles electrodes modified with RGO and Pt nanoparticles used for electrochemical treatment of azo dye. J. Electroanal. Chem. 887, 115154.

Hapeman-Somich, C.J., Zong, G., Lusby, W.R., Muldoon, M.T., Waters, R., 1992. Aqueous ozonation of atrazine. Product identification and description of the degradation pathway. J. Agric. Food Chem. 40, 2294–2298.

Hayes, T.B., Khoury, V., Narayan, A., Nazir, M., Park, A., Brown, T., Adame, L., Chan, E., Buchholz, D., Stueve, T., 2010. Atrazine induces complete feminization and chemical castration in male African clawed frogs (Xenopus laevis). Proc. Natl. Acad. Sci. Unit. States Am. 107, 4612–4617.

He, H., Liu, Y., You, S., Liu, J., Xiao, H., Tu, Z., 2019. A review on recent treatment technology for herbicide atrazine in contaminated environment. Int. J. Environ. Res. Publ. Health 16, 5129. https://doi.org/10.3390/ijerph16245129.

Hildebrandt, A., Guillamón, M., Lacorte, S., Tauler, R., Barceló, D., 2008. Impact of pesticides used in agriculture and vineyards to surface and groundwater quality (North Spain). Water Res. 42, 3315–3326.

Hou, X., Huang, X., Ai, Z., Zhao, J., Zhang, L., 2017. Ascorbic acid induced atrazine degradation. J. Hazard Mater. 327, 71–78.

Komtchou, S., Dirany, A., Drogui, P., Robert, D., Lafrance, P., 2017. Removal of atrazine and its by-products from water using electrochemical advanced oxidation processes. Water Res. 125, 91–103.

Li, D., Kaner, R.B., 2008. Graphene-based materials. Science 320, 1170–1171.

Li, Y., Gao, W., Ci, L., Wang, C., Ajayan, P.M., 2010. Catalytic performance of Pt nanoparticles on reduced graphene oxide for methanol electro-oxidation. Carbon 48, 1124–1130.

Liu, G., Yang, X., Li, T., She, Y., Wang, S., Wang, J., Zhang, M., Jin, F., Jin, M., Shao, H., 2015. Preparation of a magnetic molecularly imprinted polymer using g-C3N4–Fe3O4 for atrazine adsorption. Mater. Lett. 160, 472–475.

Luo, C., Jiang, J., Guan, C., Ma, J., Pang, S., Song, Y., Yang, Y., Zhang, J., Wu, D., Guan, Y., 2017. Factors affecting formation of diethyl and diisopropyl products from atrazine degradation in UV/H 2 O 2 and UV/PDS. RSC Adv. 7, 29255–29262.

Luo, Z., Yuwen, L., Bao, B., Tian, J., Zhu, X., Weng, L., Wang, L., 2012. One-pot, low-temperature synthesis of branched platinum nanowires/reduced graphene oxide (BPtNW/RGO) hybrids for fuel cells. J. Mater. Chem. 22, 7791–7796.

Lutze, H.V., Bircher, S., Rapp, I., Kerlin, N., Bakkour, R., Geisler, M., von Sonntag, C., Schmidt, T.C., 2015. Degradation of chlorotriazine pesticides by sulfate radicals and the influence of organic matter. Environ. Sci. Technol. 49, 1673–1680.

Ma, W.T., Fu, K.K., Cai, Z., Jiang, G.B., 2003. Gas chromatography/mass spectrometry applied for the analysis of triazine herbicides in environmental waters. Chemosphere 52, 1627–1632.

MacLennan, P., Delzell, E., Sathiakumar, N., Myers, S., 2003. Mortality among triazine herbicide manufacturing workers. J. Toxicol. Environ. Health 66, 501–517.

Malpass, G.R., Salazar-Banda, G.R., Miwa, D.W., Machado, S.A., Motheo, A.J., 2013. Comparing atrazine and cyanuric acid electro-oxidation on mixed oxide and boron-doped diamond electrodes. Environ. Technol. 34, 1043–1051.

Malpass, G.R.P., Miwa, D.W., Machado, S.A.S., Olivi, P., Motheo, A.J., 2006. Oxidation of the pesticide atrazine at DSA® electrodes. J. Hazard Mater. 137, 565–572.

Mamián, M., Torres, W., Larmat, F.E., 2009. Electrochemical degradation of atrazine in aqueous solution at a platinum electrode. Port. Electrochim. Acta 27, 371–379.

Murugananthan, M., Latha, S.S., Raju, G.B., Yoshihara, S., 2011. Role of electrolyte on anodic mineralization of atenolol at boron-doped diamond and Pt electrodes. Separ. Purif. Technol. 79, 56–62.

Nie, R., Wang, J., Wang, L., Qin, Y., Chen, P., Hou, Z., 2012. Platinum supported on reduced graphene oxide as a catalyst for hydrogenation of nitroarenes. Carbon 50, 586–596.
Oturan, N., Brillas, E., Oturan, M.A., 2012. Unprecedented total mineralization of atrazine and cyanuric acid by anodic oxidation and electro-Fenton with a boron-doped diamond anode. Environ. Chem. Lett. 10, 165–170.
Panizza, M., 2010. I. Mportance of Electrode Material in the Electrochemical Treatment of Wastewater Containing Organic Pollutants. Electrochemistry for the Environment. Springer, pp. 25–54.
Panizza, M., Cerisola, G., 2009. Direct and mediated anodic oxidation of organic pollutants. Chem. Rev. 109, 6541–6569.
Radjenovic, J., Sedlak, D.L., 2015. Challenges and opportunities for electrochemical processes as next-generation technologies for the treatment of contaminated water. Environ. Sci. Technol. 49, 11292–11302.
Reilly, T.J., Smalling, K.L., Orlando, J.L., Kuivila, K.M., 2012. Occurrence of boscalid and other selected fungicides in surface water and groundwater in three targeted use areas in the United States. Chemosphere 89, 228–234.
Ren, F., Wang, H., Zhai, C., Zhu, M., Yue, R., Du, Y., Yang, P., Xu, J., Lu, W., 2014. Clean method for the synthesis of reduced graphene oxide-supported PtPd alloys with high electrocatalytic activity for ethanol oxidation in alkaline medium. ACS Appl. Mater. Interfaces 6, 3607–3614.
Santos, T.É.S., Silva, R.S., Meneses, C.T., Martínez-Huitle, C.A., Eguiluz, K.I., Salazar-Banda, G.R., 2016. Unexpected enhancement of electrocatalytic nature of Ti/(RuO2)x–(Sb2O5)y anodes prepared by the ionic liquid-thermal decomposition method. Ind. Eng. Chem. Res. 55, 3182–3187.
Su, Y.-H., Zhu, Y.-G., 2006. Bioconcentration of atrazine and chlorophenols into roots and shoots of rice seedlings. Environ. Pollut. 139, 32–39.
Wang, Y., Li, Y., Tang, L., Lu, J., Li, J., 2009. Application of graphene-modified electrode for selective detection of dopamine. Electrochem. Commun. 11, 889–892.
Yan, L., Wang, Y., Li, J., Ma, H., Liu, H., Li, T., Zhang, Y., 2014. Comparative study of different electrochemical methods for petroleum refinery wastewater treatment. Desalination 341, 87–93.
Zaviska, F., Drogui, P., Blais, J.-F., Mercier, G., Lafrance, P., 2011. Experimental design methodology applied to electrochemical oxidation of the herbicide atrazine using Ti/IrO2 and Ti/SnO2 circular anode electrodes. J. Hazard Mater. 185, 1499–1507.
Zhou, M., Särkkä, H., Sillanpää, M., 2011. A comparative experimental study on methyl orange degradation by electrochemical oxidation on BDD and MMO electrodes. Separ. Purif. Technol. 78, 290–297.